Supplementary Information

Exploring the Programmability of Autocatalytic Chemical Reaction Networks

Dmitrii V. Kriukov,[1,2] Jurriaan Huskens,[1] Albert S. Y. Wong[1,2]*

[1] Department of Molecules and Materials, Faculty of Science and Technology & MESA+ Institute, University of Twente, Enschede, the Netherlands.

[2] BRAINS (Center for Brain-inspired Nano Systems), University of Twente, the Netherlands.

*Corresponding author. Email: albert.wong@utwente.nl

The PDF file includes:

- A detailed description of the assumptions on which the mathematical model was build, criteria for distinguishing logic gates, and a description of the validation observed history dependency in the XOR gate.
- Scripts 1, Scripts 2, Scripts 3 are provided as **Supplementary Materials**
- **Supplementary Fig. 1**
- **Supplementary Table S1**

Mathematical modelling

Our mathematical model uses ordinary differential equations (*compdeq*) and quadratic equations (*compsqeq*) to simulate reaction trajectories of our network in flow. The model (*comp*) recalculates equilibrium concentrations of forming complexes (*compsqeq*) after each iteration of 1 second of numerical solution of the CRN course (*compdeq*). The model is designed for computation of steady state and transient concentrations of Tr in the presence of different initial concentrations of species at different flowrates with different inflow concentrations of species. The list of reactions and complexes used can be found in **Supplementary Table S1**. All kinetic and thermodynamic constants were estimated from published data[30-33] to explain experimental results.

The following assumptions were used to describe the CRN (see **Scheme 1**):

1) Degradation of *Tr* and *Tg* is not a significant factor in our system as soon as residence times are way lower (typically 2-20 minutes) than half-life of species (100-200 minutes see **Extended data Fig. 4**) under examined range of concentration of ions. So, all degradation processes are not included into the model. Therefore, the model is not applicable for simulation of batch reactions.
2) There are two bindings sites for ions for *Tg*. One is called TAP (trypsinogen activation peptide), another one – pocket. Only Nd^{3+} and Ca^{2+} can bind TAP site (Nd*Tg*X; Ca*Tg*X) with K_{ng1} and K_{cg1} equilibrium constants. The cause of such difference between La and Nd lies in their different affinity (Nd binds stronger) towards a second ion-binding site of protein, which saturation slows down the reaction rate.
3) Nd^{3+}, Ca^{2+} and La^{3+} can bind to the pocket of *Tg* to form X*Tg*Nd; X*Tg*Ca; X*Tg*La with Kng2, Kcg2 and Klg2 equilibrium constants. Occupation of one site does not influence binding to the other site.
4) When TAP site of *Tg* is occupied by Nd^{3+}, the autocatalysis is not possible, otherwise (Ca^{2+} or nothing is bound) the reaction rate depends exclusively on the type of ion bound to *Tr*.
5) There is one binding site for ions for *Tr*. Nd^{3+}, Ca^{3+} and La^{3+} can bind to this binding site (*Tr*Nd; *Tr*Ca; *Tr*La) with K_{nr2}, K_{cr2} and K_{lr2} equilibrium constants. Reaction rate (k_n, k_c, k_l) depends on the ion that is bound to *Tr*.
6) Soybean Trypsin Inhibitor, STI, forms a complex only with free *Tr*.
7) We consider that the Michaelis-Menten approximation cannot be applied to *Tg* autocatalysis. Our findings in **Extended data Fig. 3** shows that Nd^{3+} influences on the autocatalytic process by changing both K_M and V_{max} nonlinearly. Rather than applying the Michaelis-Menten approach, we treat this conversion as a simple bimolecular reaction.

Supplementary Scripts

- **Scripts 1** are provided in the supplementary materials and can be used for obtaining the simulated data **Fig.4d** and **Extended Data Fig.7**.
- **Scripts 2** are provided in the supplementary materials and can be used for obtaining the simulated data **Extended Data Fig.5**.
- **Scripts 3** are provided in the supplementary materials and can be used for obtaining the simulated data **Extended Data Fig.9b.**

Criteria for distinguishing logic gates

The criteria for claiming the [Tr]* as FALSE or TRUE is the ratio between $[Tr]^*_{X|X}$ values for different $[Nd]_{X|X}$. For AND, OR and XOR the ratio between $[Tr]^*_{1|1}$ and $[Tr]^*_{1|0}$ was used. For AND gate the ratio is higher than 3, what means that $[Tr]^*_{1|1}$ is at least three times higher than $[Tr]^*_{1|0}$. For OR gate the ratio lies between 0.75 and 1.25, indicating that values for $[Tr]^*_{1|1}$ and $[Tr]^*_{1|0}$ are close. For XOR gate the ratio is lower than 0.33, what means that $[Tr]^*_{1|1}$ is at least three times lower than $[Tr]^*_{1|0}$. For NAND and NOR different ratio was implemented because $[Tr]^*_{0|0}$ for these gates is not close to 0 – sum of $[Tr]^*_{1|1}$ and $[Tr]^*_{1|0}$ against $[Tr]^*_{0|0}$. For NAND gate the ratio is between 0.75 and 1.25, indicating that the sum of $[Tr]^*_{1|0}$ and $[Tr]^*_{1|1}$ is close to $[Tr]^*_{0|0}$ (XNOR is probably impossible to achieve with our type of nonlinearity). For NOR gate the ratio is lower than 0.5, indicating that the sum of $[Tr]^*_{1|0}$ and $[Tr]^*_{1|1}$ values is at least twice lower than $[Tr]^*_{0|0}$.

Validation of history dependency

Notably, the response in the XOR gate (main text, Fig. 4B) depended on the response from the previous state ($[Nd^{3+}]_{0|0}$ or $[Nd^{3+}]_{1|1}$), indicating that the autocatalytic network is inherently history dependent. Building on this phenomenon, **Extended Data Fig. 9** demonstrates how the transition from $[Nd^{3+}]_0$ = 0 mM to $[Nd^{3+}]_0$ = 1.0 mM resulted in the typical autocatalytic production of [*Tr*] but that the inverse transition gave rise to a 'pulse'—a temporary increase in [*Tr*] before it slowly decreased to the [*Tr*] corresponding to $[Nd^{3+}]_0$=0 mM. We executed this sequence (0;1;0 mM, with steps of 30 min) three times to verify that the pulse could indeed be established reproducibly. We used our model to examine its dependence of the range of $[Nd^{3+}]_0$ as well as the differences between the maxima and minima. We classified the existence of the pulse by two variables (pulse halfwidth (parameter a, min), and pulse amplitude (parameter b, mM)). Particularly, **Extended Data Fig. 9b** shows that both variables scale with the residence time, but that the amplitude slowly diminishes if the residence time becomes higher than 8 min and for the pulse halfwidth after 5 minutes. That is, the XOR gate (and perhaps other logic gates) is history dependent under optimal residence time.

Non textual Elements.

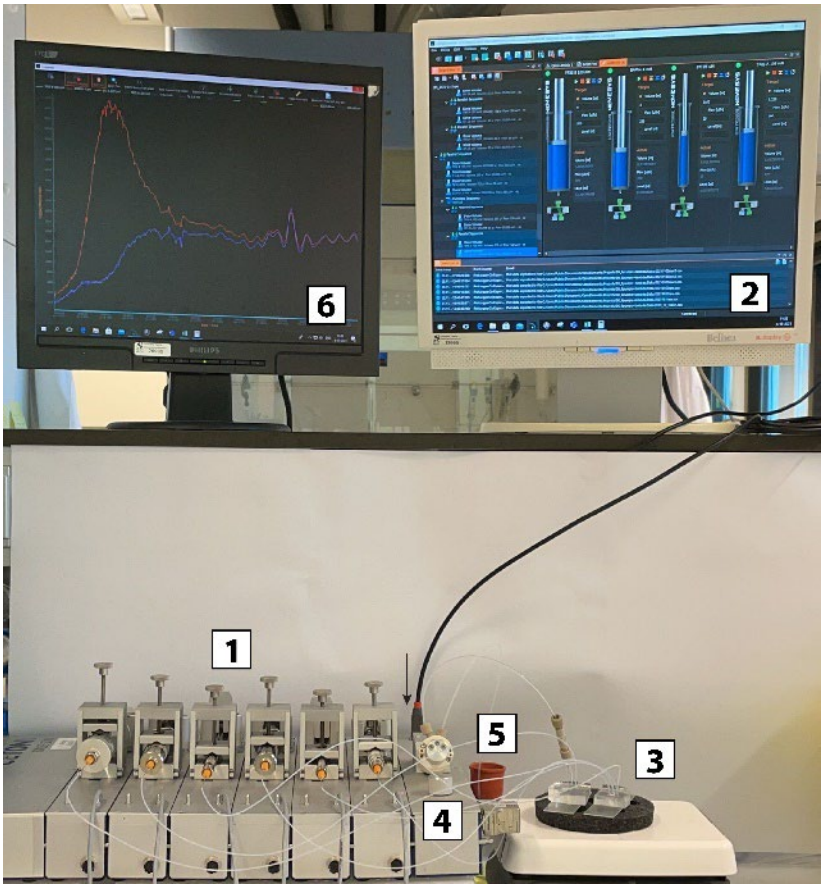

Supplementary Fig. 1: Experimental setup. 1. Glass syringes mounted on a low-pressure pump setup. 2. Pumps control program. 3. Set of CSTRs on a stirring plate. 4. Qmix Lambda flow absorbance detector. 5. Waste container. 6. Online absorbance data. Trypsin formed during autocatalytic reaction in CSTR 1 goes to CSTR 2 where BAPNA converts to pNA and overall outflow goes through flow absorbance detector.

Supplementary Table 1. The list of constants used for the model. See **Scripts** and **Supplementary Information** *Mathematical modelling* section for further details.

Reaction	Rate constant	Value L/(mol*s)	Complex	Association constant	Value L/mol
TrCa + Tg -> TrCa + Tr	kc	2E+01	Ca + Tg <-> CaTg	Kcg1	4E+01
TrCa + CaTg -> TrCa + Tr + Ca			Ca + TgCa <-> CaTgCa		
TrCa + TgCa -> TrCa + TrCa			Ca + TgNd <-> CaTgNd		
TrCa + CaTgCa -> TrCa + TrCa + Ca			Ca + TgLa <-> CaTgLa		
TrCa + TgNd -> TrCa + TrNd			Ca + Tg <-> TgCa	Kcg2	6.3E+03
TrCa + CaTgNd -> TrCa + TrNd + Ca			Ca + NdTg <-> NdTgCa		
TrCa + TgLa -> TrCa + TrLa			Ca + CaTg <-> CaTgCa		
TrCa + CaTgLa -> TrCa + TrLa + Ca			Ca + Tr <-> TgCa	Kcr	1.2E+02
TrNd + Tg -> TrNd + Tr	kn	1.8E+02	Nd + Tg <-> NdTg	Kng1	8E+03
TrNd + CaTg -> TrNd + Tr + Ca			Nd + TgCa <-> NdTgCa		
TrNd + TgCa -> TrNd + TrCa			Nd + TgNd <-> NdTgNd		
TrNd + CaTgCa -> TrNd + TrCa + Ca			Nd + TgLa <-> NdTgLa		
TrNd + TgNd -> TrNd + TrNd			Nd + Tg <-> TgNd	Kng2	1.1E+05
TrNd + CaTgNd -> TrNd + TrNd + Ca			Nd + CaTg <-> CaTgNd		
TrNd + TgLa -> TrNd + TrLa			Nd + NdTg <-> NdTgNd		
TrNd + CaTgLa -> TrNd + TrLa + Ca			Nd + Tr <-> TrNd	Knr	1.2E+04
TrLa + Tg -> TrLa + Tr	kl	4E+04	La + Tg <-> TgLa	Klg2	7.5E+05
TrLa + CaTg -> TrLa + Tr + Ca			La + CaTg <-> CaTgLa		
TrLa + TgCa -> TrLa + TrCa			La + NdTg <-> NdTgLa		
TrLa + CaTgCa -> TrLa + TrCa + Ca			La + Tr <-> TrLa	Klr	7.5E+02
TrLa + TgNd -> TrLa + TrNd			Tr + STI <-> TrSTI	Ksti	1E+09
TrLa + CaTgNd -> TrLa + TrNd + Ca					
TrLa + TgLa -> TrLa + TrLa					
TrLa + CaTgLa -> TrLa + TrLa + Ca					